

The Vibration–Rotational Bands ν_3 , $2\nu_3 - \nu_3$, and $\nu_3 + \nu_6 - \nu_6$ of H_3^{12}CF

D. PAPOUŠEK AND J. F. OGILVIE

Academia Sinica, Institute of Atomic and Molecular Sciences, P.O. Box 23-166, Taipei 10764, Taiwan

AND

S. ČIVIŠ¹ AND M. WINNEWISSER

*Physikalisch-Chemisches Institut, Justus-Liebig, Universität Giessen, Heinrich-Buff-Ring 58,
W-6300 Giessen, Federal Republic of Germany*

The vibration–rotational bands ν_3 , $2\nu_3 - \nu_3$, and $\nu_3 + \nu_6 - \nu_6$ of gaseous fluoromethane H_3^{12}CF in the $10\ \mu\text{m}$ region have been measured in absorption on an interferometric spectrometer with spectral resolution $0.002\ \text{cm}^{-1}$. Simultaneously with 95 previously reported frequencies of pure rotational transitions in the ground vibrational state and 55 rotational transitions in the excited vibrational state $\nu_3 = 1$, the wavenumbers of 1161 vibration–rotational transitions of the ν_3 band and of 502 vibration–rotational transitions of the band $2\nu_3 - \nu_3$ have been fitted to determine 14 parameters of the ν_3 band and 13 parameters of the band $2\nu_3 - \nu_3$ which describe the infrared data with a standard deviation $5.6 \times 10^{-5}\ \text{cm}^{-1}$. For possible use as secondary standards for wavenumber calibration, 290 selected lines of the fundamental band are listed in the range $958\text{--}1097\ \text{cm}^{-1}$. The wavenumbers of 614 lines of the “hot” band $\nu_3 + \nu_6 - \nu_6$ have been used to determine 15 parameters of this band which describe the experimental data with a standard deviation $7.6 \times 10^{-5}\ \text{cm}^{-1}$. Opposite signs of the effective coefficients of the “2, 2” *l*-type interaction in the vibrational states $|v_3, \nu_6^k\rangle = |0, 1^{\pm 1}\rangle$ and $|1, 1^{\pm 1}\rangle$ of H_3^{12}CF have been explained by different coupling schemes for the x - y Coriolis interactions affecting the states $|0, 1^{\pm 1}\rangle$ and $|1, 1^{\pm 1}\rangle$. © 1991 Academic Press, Inc.

INTRODUCTION

Fluoromethane H_3CF has proved a suitable chemical compound for various spectroscopic experiments with lasers, including generation of submillimeter-wave coherent radiation in optically pumped lasers and studies of transfer of collisional energy. These experiments are based on the near coincidence of the wavenumbers of the vibration–rotational transitions with the wavenumbers of lines from CO_2 lasers. The vibration–rotational spectrum of H_3CF has hence been the subject of several spectral investigations at high resolution [cf. Refs. (1, 2) and references therein]. Schwendeman and co-workers (1, 2) have recently measured spectra with an infrared-microwave sideband laser to investigate the three vibration–rotational bands which appear in the $10\ \mu\text{m}$

¹ Present address: J. Heyrovský Institute of Physical Chemistry and Electrochemistry, Dolejškova 3, 182 23 Prague 8, Czechoslovakia.

region: the bands ν_3 , $2\nu_3 - \nu_3$, and $\nu_3 + \nu_6 - \nu_6$. Their technique provides accurate transition frequencies but their measurements were limited to lines with frequencies which are near the CO₂ laser frequencies.

Because the precision of measurements by means of interferometric spectrometers approaches the precision of the determination of frequencies by the techniques of Doppler-limited laser spectroscopy (1–3 MHz for isolated spectral lines), we have remeasured the bands ν_3 , $2\nu_3 - \nu_3$, and $\nu_3 + \nu_6 - \nu_6$ of H₃¹²CF. Our objectives were to determine more accurate parameters of these bands, to test the consistency between the infrared-microwave sideband and interferometric techniques, and to verify the possibility of a theoretical description of the frequencies of lines with values of J exceeding those which were measured previously [(1, 2); see also Table I].

EXPERIMENTAL DETAILS

The sample of H₃CF was prepared from the reaction of the methyl ester of perfluorosulfonic acid with NaF according to the method of Edgell and Parts (3). Fluoromethane was obtained by distillation at the temperature of a bath of solid CO₂ and ethanol as a fraction with boiling point 195 K. Its purity was tested by gas chromatography and mass spectrometry.

The infrared spectra were measured in absorption on an interferometric spectrometer (Bruker IFS 120 HR) at an unapodized resolution 0.0028 cm⁻¹ whereas the Doppler width in the range covered, 945–1102 cm⁻¹, is 0.0020–0.0023 cm⁻¹. The length of the absorbing path was 2.84 m. For calibration we used the measured positions of N₂O lines as previously described (4). At a temperature 300 K, the pressure of the gaseous H₃CF sample was 5 Pa for the ν_3 band and 50 Pa for the bands $2\nu_3 - \nu_3$ and $\nu_3 + \nu_6 - \nu_6$. An excerpt 1012–1014 cm⁻¹ of the spectrum is given in Fig. 1.

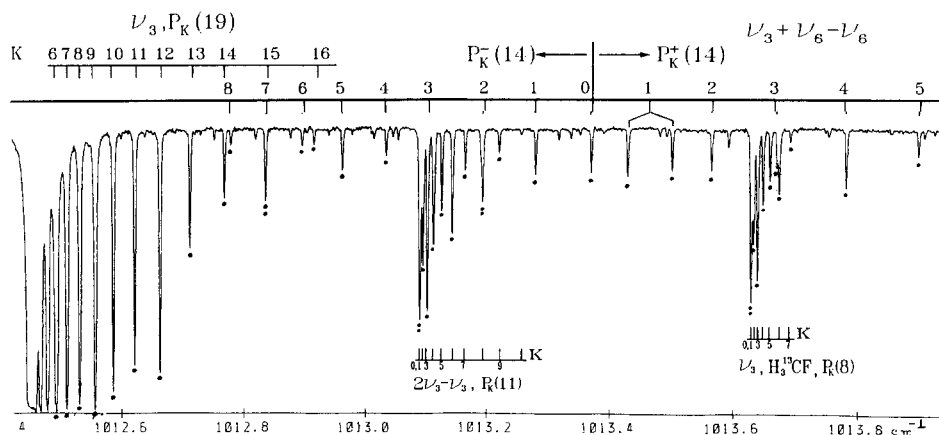


FIG. 1. Part of the spectrum of the bands ν_3 , $2\nu_3 - \nu_3$, and $\nu_3 + \nu_6 - \nu_6$ of H₃¹²CF; sample pressure was 50 Pa. ($P_K(8)$ lines of H₃¹³CF in natural abundance are also visible.)

THEORY AND ANALYSIS

The Bands ν_3 and $2\nu_3 - \nu_3$

The fundamental ν_3 band, described as the C–F stretching mode and belonging to symmetry class A_1 according to the point group C_{3v} , is a prototypical parallel band of a prolate symmetric rotor. The vibrational state $|v_3, v_6\rangle = |1, 0^0\rangle$ (this notation to denote vibrational states is used consistently hereafter) interacts with the nearest vibrational state $|0, 1^{\pm 1}\rangle (E)$ [$\nu_6 - \nu_3 = 134.06 \text{ cm}^{-1}$; see Ref. (4)] by an x – y Coriolis interaction. Moreover, the interactions with $\Delta k = \pm 3$ and $\Delta k = \pm 6$ which are diagonal in the vibrational quantum numbers can split the energies of states having $K = 3$ ($\Delta k = \pm 6$ interaction) or shift the energies of other states. However, if we suppose that the effect of the x – y Coriolis interaction is “absorbed” by the effective values of the spectral parameters, and if we neglect the interactions with $\Delta k = \pm 3, \pm 6, \dots$, the expression for the energies of the rotational states in a nondegenerate vibrational state is written in the standard polynomial form

$$\begin{aligned}
 E_{\text{vr}}(J, k)/hc = & E_v^0/hc + B_v J(J+1) + (A_v - B_v)K^2 - D_J^{(v)} J^2(J+1)^2 \\
 & - D_{JK}^{(v)} J(J+1)K^2 - D_K^{(v)} K^4 + H_J^{(v)} J^3(J+1)^3 + H_{JK}^{(v)} J^2(J+1)^2 K^2 \\
 & + H_{KJ}^{(v)} J(J+1)K^4 + H_K^{(v)} K^6 + L_J^{(v)} J^4(J+1)^4 + L_{JK}^{(v)} J^3(J+1)^3 K^2 \\
 & + L_{JK}^{(v)} J^2(J+1)^2 K^4 + L_{JKK}^{(v)} J(J+1)K^6 + L_K^{(v)} K^8 + \dots \quad (1)
 \end{aligned}$$

We assume that Eq. (1) holds for not only $|1, 0^0\rangle$ (and the ground vibrational state) but also the state $|2, 0^0\rangle$. Whether these approximations are good (and, ultimately, within which range of values of J) must of course be decided for each individual molecular species.

The standard selection rules are $\Delta J = 0, \pm 1$; $\Delta K = 0$ for the vibration–rotational transitions and $\Delta J = +1, \Delta K = 0$ for the pure rotational transitions within the vibrational states $|0, 0^0\rangle$ (or ground), $|1, 0^0\rangle$. We have applied Eq. (1) and these selection rules in a simultaneous least-squares fit to 1161 vibration–rotational transitions of the ν_3 band, 502 vibration–rotational transitions of the band $2\nu_3 - \nu_3$, 95 previously reported frequencies of the pure rotational transitions within the ground vibrational state [cf. Ref. (4) and references therein], and 55 rotational transitions within the excited vibrational state $|1, 0^0\rangle (I)$. The range of quantum numbers probed with these data is shown in Table I. The resulting 14 parameters of the band ν_3 and 13 parameters of the band $2\nu_3 - \nu_3$ are listed in Table II. The data were weighted according to the inverse square, $(\Delta\nu)^{-2}$, of the estimated experimental uncertainty $\Delta\nu$ of the lines. The uncertainties of the vibration–rotational lines were estimated to be 1 MHz for isolated lines with good ratio of signal to noise, but greater for less intense lines or lines the positions of which were influenced by other lines in more or less near coincidence. Lines with uncertainties exceeding $3 \times 10^{-3} \text{ cm}^{-1}$ were excluded from the fit. The greater accuracy of the microwave and submillimeter-wave data for the pure rotational transitions ($\Delta\nu < 0.1 \text{ MHz}$) in the states $|0, 0^0\rangle$ and $|1, 0^0\rangle$ by comparison with the infrared data prevails in the determination of the spectral parameters at small values of J . We have thus determined improved values of the parameters for the ν_3

TABLE I

Survey of Lines Measured in the Bands ν_3 , $2\nu_3 - \nu_3$, and $\nu_3 + \nu_6 - \nu_6$ of H_3^{12}CF

Band	Branch	J_{max}		No. of data	s.d. ^b
		Previous work ^a	This work		
ν_3	P	30	47	1161	5.6×10^{-5}
	Q	39	34		
	R	23	46		
$2\nu_3 - \nu_3$	P	7	31	502	
	Q	23	20		
	R	17	31		
$\nu_3 + \nu_6 - \nu_6$	P ⁺	17	27	614	7.6×10^{-5}
	Q ⁺	19	7		
	R ⁺	20	26		
	P ⁻	17	26		
	Q ⁻	17	10		
	R ⁻	20	27		

^a See Ref. (1) for bands ν_3 and $2\nu_3 - \nu_3$ and Ref. (2) for the band $\nu_3 + \nu_6 - \nu_6$.^b Standard deviation/cm⁻¹.

band, especially such parameters as D_J , H_J , H_{JK} , L_J , and L_{JJJK} ; the lines corresponding to greater values of J accessible in our infrared measurements (cf. Table I) made the latter quantities more important. Substantially improved values have of course been obtained for all parameters of the band $2\nu_3 - \nu_3$ of H_3^{12}CF .

Neither systematic deviations between the calculated and experimental wavenumbers nor splittings between A_1 and A_2 states have been observed in the band ν_3 or $2\nu_3 - \nu_3$ in the entire range of values of the rotational quantum numbers in Table I, which for the ν_3 band is almost a unique feature of H_3CF .

The Band $\nu_3 + \nu_6 - \nu_6$

As noted in previous work (2), the band $\nu_3 + \nu_6 - \nu_6$ is of interest because it is due to transitions between two doubly degenerate vibrationally excited states. Furthermore, the coefficients of the "2, 2" l -type interaction were found to have opposite signs in the states $|0, 1^{\pm 1}\rangle$ and $|1, 1^{\pm 1}\rangle$ (2), for which an explanation is required. We have remeasured this band not only because lines with values of J greater than in the previous study (2) were accessible to us but also because both pure rotational transitions in the state $v_6 = 1$ of H_3^{12}CF (5, 6) and the ν_6 band (4) have been recently measured.

As in our previous study of the ν_6 band, we have assumed that all the vibration-rotational interactions off-diagonal in the principal vibrational quantum numbers v can be taken adequately into account by the effective values of the spectral parameters of the states $|0, 1^{\pm 1}\rangle$ and $|1, 1^{\pm 1}\rangle$. The expression for the vibration-rotational terms is then written

$$E_{\text{vrl}}(J, k; l)/hc = E_{\text{vr}}/hc + [-2(A_{\zeta^2}^{\pm})_v Kl + \eta_J J(J+1)Kl + \eta_K K^3 l + \tau_J J^2(J+1)^2 Kl + \tau_{JK} J(J+1)K^3 l + \tau_K K^5 l + \dots] + E_{\text{off-d}}/hc \quad (2)$$

TABLE II
Vibration-Rotational Parameters/cm⁻¹ of the Vibrational States $|v_3, v_6\rangle = |0, 0^0\rangle$, $|1, 0^0\rangle$, and $|2, 0^0\rangle$ of H₃¹²CF

Parameter ^a	$ 0, 0^0\rangle$		$ 1, 0^0\rangle$		$ 2, 0^0\rangle$	
	This work	Ref. (1)	This work	Ref. (1)	This work	Ref. (1)
E_0^b/hc	0		1048.610701(10)	1048.610639(10)	2081.380386(26)	2081.380179(33)
F_V	0.851794269(18)	0.851794274(20)	0.840498482(29)	0.840498436(33)	0.829608856(281)	0.829606661(1300)
$\Delta(A_V - B_V)/10^{-3}$	0 ^c		1.48074(64)	1.47946(66)	2.71791(192)	2.71191(350)
$D_J/10^{-6}$	2.00877(7)	2.00916(12)	1.89754(11)	1.89727(20)	1.82013(83)	1.78287(350)
$D_{JK}/10^{-6}$	14.67037(81)	14.66262(104)	17.28658(157)	17.28139(164)	19.07549(1480)	19.21839(3380)
$\Delta D_K/10^{-6}$	0 ^c		-3.12018(1120)	-3.13602(1020)	-5.29295(3590)	-5.65878(9990)
$H_J/10^{-9}$	-0.001072(31)	-0.000727(23)	-0.006452(98)	-0.007839(407)	-0.00697(67)	-0.22252(3690)
$H_{JK}/10^{-9}$	0.064946(918)	0.058434(2530)	0.536266(1720)	0.531905(4260)	0.90711(3250)	1.92349(17500)
$H_{KJ}/10^{-9}$	0.745882(5340)	0.722763(6410)	-3.217208(16200)	-3.080154(22700)	-4.85635(20600)	-6.92979(64300)
$\Delta H_K/10^{-9}$	0 ^d	0 ^d	3.995669(75900)	3.550603(56000)	7.14335(18300)	5.76232(123000)
$L_J/10^{-12}$	0 ^d	0 ^d	0.000339(29)	0.002098(200)	0 ^d	0.27966(50400)
$L_{JK}/10^{-12}$	0 ^d	0 ^d	-0.058266(624)	-0.095726(2490)	-0.14740(2250)	-1.55111(48100)
$L_{JK}/10^{-12}$	0 ^d	0 ^d	0.986176(7130)	1.375288(15900)	0.94347(18500)	3.56256(159000)
$L_{JKK}/10^{-12}$	0 ^d	0 ^d	-5.778548(48900)	-7.915172(62500)	-10.24190(88500)	-7.95851(181000)
$\Delta L_K/10^{-12}$	0 ^d	0 ^d	0 ^d	5.170494(105000)	0 ^d	4.75706(331000)

^a Definition of notation: $\Delta P = P(v) - P(0)$.

^b Figures in parentheses are standard errors (rounded) in units of the last digit stated. To facilitate comparison with our results, we converted values from Ref. (2) into cm⁻¹ units; some values are reproduced here to more digits than in Ref. (2).

^c According to Graner (9), $A_0 = 5.182009(12)$ cm⁻¹, $D_K^0 = 70.33(25) \times 10^{-6}$ cm⁻¹.

^d Constrained to zero.

in which E_{vr} is formally defined as in Eq. (1), $l = +1$ for the $+l$ levels and $l = -1$ for the $-l$ levels of the state $|0, 1^{\pm 1}\rangle$ or $|1, 1^{\pm 1}\rangle$. The only interaction which leads to an observable off-diagonal contribution is the "2,2" l -type interaction which may be represented by a diagonal contribution to the level $kl = +1$ of the state $|0, 1^{\pm 1}\rangle$ or $|1, 1^{\pm 1}\rangle$ [cf. Ref. (4)]:

$$\langle A_{\pm} | (H_{22} + H_{24}) / hc | A_{\pm} \rangle [= E_l(J, Kl = +1) / hc] \\ = \pm 2 [q_v^* + f_v^{(J)} J(J+1)] J(J+1), \quad (3)$$

in which $q_v^* = q_v + 2f_v^{(K)}$ is a determinable parameter; in terms of the basis functions $|v_3, v_6^k; J, k\rangle$, one obtains

$$|A_{\pm}\rangle = 2^{-1/2} [|v_3, v_6^k = 1^{+1}; J, +1\rangle \pm |v_3, v_6^k = 1^{-1}; J, -1\rangle], \quad (4)$$

for $v_3 = 0$ or 1 . For $kl \neq 1$, a treatment according to perturbation theory up to second order yields a correction to the energies

$$E_l^{(v)}(J, K, \pm l) = \pm [q_v^* + f_v^{(J)} J(J+1) + 2f_v^{(K)} K^2]^2 [J(J+1)] \\ \times [J(J+1) - (K \mp 1)(K \mp 2)] / [A_v - B_v - (A \xi_v^{\pm})] (K \mp 1) \quad (5)$$

in which all signs on both sides of Eq. (5) are correlated. Note that, although the analogous formula in Ref. (2) is incorrect, calculations in Ref. (2) were obviously made with the correct expression. Note also that by definition our parameters q and f are one-quarter of those defined in Ref. (2).

Before we discuss in detail the relative signs of the effective values of the "2,2" l -type interaction in the states $|0, 1^{\pm 1}\rangle$ and $|1, 1^{\pm 1}\rangle$, we emphasize here that the sign of the coefficient q_v as such depends on the arbitrary phase conventions used to define the wavefunctions. Thus the sign relations in Eq. (3) depend on the definition of the stabilized wavefunctions $|A_{\pm}\rangle$ in Eq. (4) and on the phase conventions implicitly involved in the evaluation of the matrix elements of the "2,2" l -type interaction in Ref. (8) which were also adopted in this paper [see Refs. (10, 11) for the comprehensive discussion of the effect of phase conventions].

The selection rules for allowed transitions between the doubly degenerate vibrational states $|0, 1^{\pm 1}\rangle$ and $|1, 1^{\pm 1}\rangle$ are $\Delta J = 0, \pm 1$; $\Delta K = 0$. Moreover, we have the selection rule $+l \leftrightarrow +l, -l \leftrightarrow -l$ for transitions between the states the energies of which for $K \neq 0$ are split by the Coriolis interaction for rotation about the z axis (7).

The symmetry species of the rovibronic wavefunctions are A_1 or A_2 for the $+l$ levels with the rotational quantum numbers $3K + 1$ ($K = 0, 1, 2, \dots$), otherwise E . For the $-l$ levels, the species are A_1 or A_2 for $3K + 2$, otherwise E . The spin-statistical weights are 4 for the states with the overall species A_1 or A_2 and 4 for the E species. The characteristic pattern of the band $\nu_3 + \nu_6 - \nu_6$ is discernible in Fig. 1. For each value of J in the P branch, the transitions with $\Delta J = -1$ from the state $|0, 1^{\pm 1}\rangle, +l$ [denoted $P_K^+(J)$ lines] extend to larger wavenumbers whereas those originating from the state $|0, 1^{\pm 1}\rangle, -l$ [$P_K^-(J)$ lines] extend to smaller wavenumbers relative to the $P_0^{\pm}(J)$ line. If the splitting of the lines corresponding to transitions between the states of the overall symmetry A_1 and A_2 is unresolved, the combined line appears with approximately twice the intensity of E transitions [see, e.g., $P_4^+(14)$ or $P_5^+(14)$ in Fig. 1]. We were actually able to observe the splitting of A_1, A_2 lines only with $kl = 1$

[“giant” l -type splitting, for instance, the line $P_1^+(14)$ in Fig. 1]. We observed a minute splitting of the lines for states with $kl = -2$ for the largest values of J , but the magnitude of the splitting and the intensity of the lines were so small that we attempted no fits to determine the coefficient of the interaction with $\Delta l = \pm 2$, $\Delta k = \mp 4$ [cf. Ref. (4)].

We have fitted 614 lines (cf. Table I) to determine 15 parameters of the band $\nu_3 + \nu_6 - \nu_6$ which are listed in Table III. These parameters reproduce the experimental data with a standard deviation $7.6 \times 10^{-5} \text{ cm}^{-1}$. The parameters of the state $|0, 1^{\pm 1}\rangle$ taken from our previous report (4) are given for comparison in the final column of Table III. The parameters of the band $\nu_3 + \nu_6 - \nu_6$ that we have determined are certainly more accurate than those obtained previously (2); in most cases the latter values fall outside our error intervals. This effect is explained first by the fact that we used different (and much more precise) values for parameters of the state $|0, 1^{\pm 1}\rangle$. Second, we had access to lines with greater values of J than were available in the previous work (2); indeed, we used about four times as many lines in our fit as in Ref. (2). Third, we constrained to zero the parameter ΔL_K , which affects the values of other parameters in the polynomial.

A complete list of the giant l -type splittings in the $\nu_3 + \nu_6 - \nu_6$ band is given in Table IV. We confirmed the opposite signs of the parameter q_v^* , which reflects these splittings, in the states $|1, 1^{\pm 1}\rangle$ and $|0, 1^{\pm 1}\rangle$ reported by Schwendeman and co-

TABLE III
Vibration-Rotational Parameters/cm⁻¹ of the Vibrational States $|v_3, v_6^l\rangle = |1, 1^{\pm 1}\rangle$
and $|0, 1^{\pm 1}\rangle$ of H₃¹²CF

Parameter ^a	$ 1, 1^{\pm 1}\rangle$		$ 0, 1^{\pm 1}\rangle$
	This work	Ref. (2)	Ref. (4)
E_v^0/hc	2221.805006(14) ^b	2221.806561(36)	1182.674392(17)
B_v	0.836652677(181)	0.836652629(1020)	0.847883432(162)
$(A_v - B_v)$	4.35245900(168)	4.35494578(320)	4.35024130(178)
$D_J/10^{-6}$	1.91813(64)	1.93721(13700)	2.02636(37)
$D_{JK}/10^{-6}$	17.46034(1090)	17.34089(12400)	15.37401(1150)
$D_K/10^{-6}$	69.53110(4380)	68.01702(7250)	72.43491(3330)
$H_J/10^{-9}$	-0.00516(66)	0.00389(285)	0.00026(9)
$H_{JK}/10^{-9}$	0.20951(1570)	0.29907(2240)	-0.1580(247)
$H_{KJ}/10^{-9}$	-3.94220(19900)	-6.23401(108000)	0.1684(999)
$\Delta H_K/10^{-9}$	0 ^c	0.4423(4240)	0 ^c
$(A\zeta^Z)_v$	1.49468058(178)	1.49603817(323)	1.54232072(311)
$\eta_J/10^{-6}$	29.6996(276)	31.4504(1440)	36.2953(592)
$\eta_K/10^{-6}$	76.8162(892)	-316.200(14)	70.2924(2440)
$\tau_J/10^{-9}$	3.431(50)	0 ^c	2.887(146)
$q_v^*/10^{-6}$	17.8874(409)	18.3854(408)	-73.1603(481)
$q_v^{(J)}/10^{-9}$	8.5211(1010)	8.0038(1730)	18.0820(637)

^a $\Delta P = P(v) - P(0)$.

^b Figures in parentheses are standard errors in units of the last digit stated.

^c Constrained to zero.

TABLE IV

Observed and Calculated Wavenumbers/cm⁻¹ of the *l*-Type Doublets (*kl* = +1) in the Band $\nu_3 + \nu_6 - \nu_6$ of H₃¹²CF^a

J	Species	EXP	CALC	(EXP-CALC)/10 ⁻⁶	UNC/10 ⁻⁶
			P ⁺ BRANCH		
2	A ₁ ->A ₂	1035.814050	1035.813142	908	1000
2	A ₂ ->A ₁	1035.814050	1035.815038	-988	1000
3	A ₂ ->A ₁	1034.071487	1034.071515	-28	300
3	A ₁ ->A ₂	1034.075278	1034.075447	-169	300
4	A ₁ ->A ₂	1032.307189	1032.307203	-14	100
4	A ₂ ->A ₁	1032.313774	1032.313890	-116	200
5	A ₂ ->A ₁	1030.519929	1030.520264	-335	500
5	A ₁ ->A ₂	1030.530788	1030.530423	365	500
6	A ₁ ->A ₂	1028.710643	1028.710761	-118	200
6	A ₂ ->A ₁	-	1028.725102	-	-
7	A ₂ ->A ₁	1026.878795	1026.878758	37	300
7	A ₁ ->A ₂	1026.898269	1026.897985	284	500
8	A ₁ ->A ₂	1025.024311	1025.024323	-12	100
8	A ₂ ->A ₁	1025.049169	1025.049132	37	100
9	A ₂ ->A ₁	1023.147506	1023.147526	-20	33
9	A ₁ ->A ₂	1023.178616	1023.178606	10	100
10	A ₁ ->A ₂	1021.248426	1021.248442	-16	33
10	A ₂ ->A ₁	1021.286501	1021.286472	29	33
11	A ₂ ->A ₁	1019.327073	1019.327146	-73	33
11	A ₁ ->A ₂	1019.372855	1019.372797	58	33
12	A ₁ ->A ₂	1017.383676	1017.383719	-43	100
12	A ₂ ->A ₁	1017.437673	1017.437649	24	300
13	A ₂ ->A ₁	1015.418209	1015.418242	-33	33
13	A ₁ ->A ₂	1015.481344	1015.481098	246	200
14	A ₁ ->A ₂	1013.430971	1013.430802	169	100
14	A ₂ ->A ₁	1013.503259	1013.503218	41	100
15	A ₂ ->A ₁	1011.421500	1011.421486	14	33
15	A ₁ ->A ₂	1011.503975	1011.504082	-107	33
16	A ₁ ->A ₂	1009.390338	1009.390384	-46	100
16	A ₂ ->A ₁	1009.483738	1009.483767	-29	100
17	A ₂ ->A ₁	1007.337537	1007.337591	-54	300
17	A ₁ ->A ₂	1007.442310	1007.442350	-40	300
18	A ₁ ->A ₂	1005.263270	1005.263202	68	500
18	A ₂ ->A ₁	1005.379867	1005.379911	-44	100
19	A ₂ ->A ₁	1003.167366	1003.167315	51	100
19	A ₁ ->A ₂	1003.295973	1003.296531	-558	*
20	A ₁ ->A ₂	1001.050047	1001.050032	15	33
20	A ₂ ->A ₁	1001.192272	1001.192293	-21	33
21	A ₂ ->A ₁	998.911618	998.911456	162	100
21	A ₁ ->A ₂	999.067239	999.067282	-43	100
22	A ₁ ->A ₂	996.751912	996.751693	219	300
22	A ₂ ->A ₁	996.921458	996.921582	-124	500

^a Lines denoted by an asterisk were excluded from the fit. The symmetry species of the initial and final states of each transition are indicated. The measured and calculated wavenumbers and their difference are indicated; UNC denotes the uncertainty of the transition wavenumber. The units of the values in the latter four columns are cm⁻¹.

TABLE IV—Continued

J	Species	EXP	CALC	(EXP-CALC)/10 ⁻⁶	UNC/10 ⁻⁶
23	A ₂ ->A ₁	994.571160	994.570850	310	1000
23	A ₁ ->A ₂	994.755276	994.755280	-4	1000
24	A ₁ ->A ₂	992.369207	992.369038	169	500
24	A ₂ ->A ₁	992.568475	992.568465	10	500
25	A ₂ ->A ₁	990.146481	990.146369	112	200
25	A ₁ ->A ₂	-	990.361227	-	-
26	A ₁ ->A ₂	987.903126	987.902956	170	200
26	A ₂ ->A ₁	988.133781	988.133655	126	300
27	A ₂ ->A ₁	-	985.638918	-	-
27	A ₁ ->A ₂	985.885421	985.885841	-420	300
Q ⁺ BRANCH					
1	A ₂ ->A ₁	1039.205671	1039.205422	249	1000
1	A ₁ ->A ₂	1039.205671	1039.205864	-193	1000
2	A ₁ ->A ₂	-	1039.160027	-	-
2	A ₂ ->A ₁	-	1039.161350	-	-
3	A ₂ ->A ₁	-	1039.091945	-	-
3	A ₁ ->A ₂	-	1039.094582	-	-
4	A ₁ ->A ₂	-	1039.001186	-	-
4	A ₂ ->A ₁	-	1039.005565	-	-
5	A ₂ ->A ₁	1038.891082	1038.887767	3315	*
5	A ₁ ->A ₂	1038.891082	1038.894304	-3222	*
6	A ₁ ->A ₂	-	1038.751707	-	-
6	A ₂ ->A ₁	-	1038.760805	-	-
7	A ₂ ->A ₁	-	1038.593029	-	-
7	A ₁ ->A ₂	-	1038.605077	-	-
R ⁺ BRANCH					
1	A ₂ ->A ₁	1042.552735	1042.551733	1002	1000
1	A ₁ ->A ₂	1042.552735	1042.552749	-14	1000
2	A ₁ ->A ₂	1044.180955	1044.179163	1792	*
2	A ₂ ->A ₁	1044.180955	1044.181780	-825	*
3	A ₂ ->A ₁	1045.783525	1045.783620	-95	1500
3	A ₁ ->A ₂	1045.788499	1045.788566	-67	1500
4	A ₁ ->A ₂	1047.365418	1047.365067	351	1000
4	A ₂ ->A ₁	-	1047.373068	-	-
5	A ₂ ->A ₁	1048.923415	1048.923471	-56	1500
5	A ₁ ->A ₂	1048.935211	1048.935250	-39	1500
6	A ₁ ->A ₂	1050.458835	1050.458799	36	33
6	A ₂ ->A ₁	1050.475080	1050.475076	4	33
7	A ₂ ->A ₁	1051.970989	1051.971025	-36	100
7	A ₁ ->A ₂	1051.992441	1051.992514	-73	33
8	A ₁ ->A ₂	1053.460115	1053.460123	-8	33
8	A ₂ ->A ₁	1053.487604	1053.487533	71	100
9	A ₂ ->A ₁	1054.925882	1054.926070	-188	100
9	A ₁ ->A ₂	1054.960114	1054.960105	9	33
10	A ₁ ->A ₂	1056.368718	1056.368848	-130	100
10	A ₂ ->A ₁	1056.410173	1056.410201	-28	100

TABLE IV—Continued

J	Species	EXP	CALC	(EXP-CALC)/10 ⁻⁶	UNC/10 ⁻⁶
11	A ₂ ->A ₁	1057.788353	1057.788439	-86	33
11	A ₁ ->A ₂	1057.837732	1057.837799	-67	33
12	A ₁ ->A ₂	1059.184775	1059.184831	-56	*
12	A ₂ ->A ₁	1059.242852	1059.242874	-22	*
13	A ₂ ->A ₁	1060.557906	1060.558013	-107	100
13	A ₁ ->A ₂	1060.625403	1060.625406	-3	33
14	A ₁ ->A ₂	1061.908575	1061.907976	599	*
14	A ₂ ->A ₁	1061.985383	1061.985376	7	33
15	A ₂ ->A ₁	1063.234724	1063.234714	10	33
15	A ₁ ->A ₂	1063.322773	1063.322765	8	33
16	A ₁ ->A ₂	1064.538240	1064.538226	14	33
16	A ₂ ->A ₁	1064.637556	1064.637559	-3	100
17	A ₂ ->A ₁	1065.818559	1065.818511	48	200
17	A ₁ ->A ₂	1065.930216	1065.929743	473	*
18	A ₁ ->A ₂	1067.075543	1067.075570	-27	300
18	A ₂ ->A ₁	1067.199395	1067.199304	91	300
19	A ₂ ->A ₁	1068.309420	1068.309409	11	33
19	A ₁ ->A ₂	1068.446176	1068.446232	-56	100
20	A ₁ ->A ₂	1069.519964	1069.520035	-71	33
20	A ₂ ->A ₁	1069.670561	1069.670517	44	100
21	A ₂ ->A ₁	1070.707550	1070.707456	94	*
21	A ₁ ->A ₂	1070.872348	1070.872149	199	*
22	A ₁ ->A ₂	-	1071.871684	-	-
22	A ₂ ->A ₁	1072.051074	1072.051123	-49	1000
23	A ₂ ->A ₁	1073.012572	1073.012733	-161	1500
23	A ₁ ->A ₂	1073.207274	1073.207432	-158	1500
24	A ₁ ->A ₂	-	1074.130617	-	-
24	A ₂ ->A ₁	1074.341100	1074.341072	28	200
25	A ₂ ->A ₁	1075.225255	1075.225354	-99	300
25	A ₁ ->A ₂	1075.451998	1075.452037	-39	*
26	A ₁ ->A ₂	1076.296824	1076.296964	-140	100
26	A ₂ ->A ₁	1076.540253	1076.540327	-74	100

workers (2), for which we offer the following explanation. The A_1 , A_2 splitting of the energies of the states with $kl = 1$ is caused both by the x - y Coriolis interaction between the vibrational states as indicated in Fig. 2 [H_{21} operator, cf. Ref. (7)] and by the diagonal contribution of the 2,2 l -type interaction [H_{22} operator]. As one can confirm by a treatment of the Coriolis interaction according to second-order perturbation theory, these contributions cannot be separated in a fit of the wavenumber data. The x - y Coriolis interaction (H_{21}) between the vibrational states $|1, 0^0\rangle$ and $|0, 1^{\pm 1}\rangle$ involves the rovibronic states $|1, 0^0; J, 0\rangle$, $|0, 1^{\pm 1}; J, +1\rangle$, and $|0, 1^{\pm 1}; J, -1\rangle$. Consequently the state

$$|A_+\rangle = 2^{-1/2}[|0, 1^{\pm 1}; J, +1\rangle + |0, 1^{\pm 1}; J, -1\rangle] \quad (6)$$

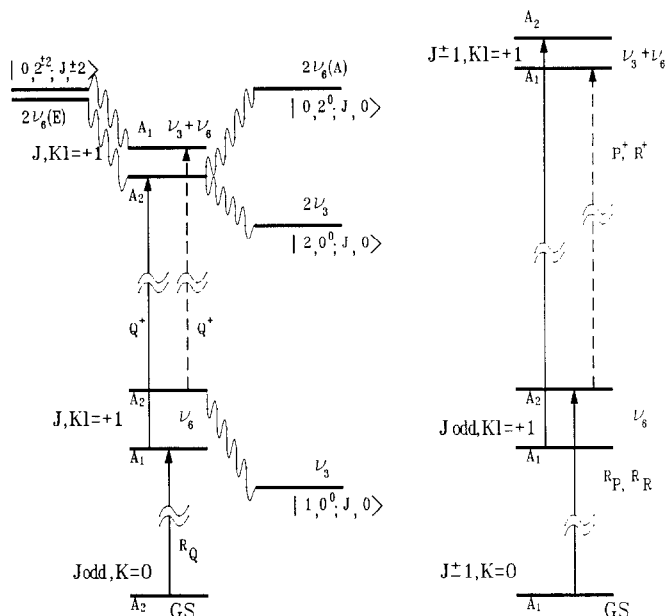


FIG. 2. Scheme of the x - y Coriolis interactions affecting the states $kl = 1$ of the vibrational states $|0, 1^{\pm 1}\rangle$ and $|1, 1^{\pm 1}\rangle$ of H₃CF. The symmetry species and allowed transitions are shown for J odd.

is unperturbed, whereas the state corresponding to $|A_- \rangle$ is shifted by approximately

$$\Delta_{\text{Cor}} = (2B\zeta_{3,6}^y \Omega_{3,6})^2 J(J+1) / [\nu_6 - \nu_3 + (A - B - A\zeta_6^z)]. \quad (7)$$

For $2B\zeta_{3,6}^y \Omega_{3,6} \cong 0.539 \text{ cm}^{-1}$ (12), this relation leads to

$$\Delta_{\text{Cor}} = 2.147 \times 10^{-3} J(J+1) \quad (8)$$

compared to

$$\Delta_{\text{exp}} = 2.926 \times 10^{-4} J(J+1) \quad (9)$$

obtained from our fit of the data (Table IV). Thus the contribution of the operator H_{22} is estimated to be

$$\Delta_{2,2} = -1.854 \times 10^{-3} J(J+1). \quad (10)$$

The situation is more complicated for the vibrational state $|1, 1^{\pm 1}\rangle$ because this state interacts with three different vibrational states as shown in Fig. 2: $|0, 2^0\rangle$, $|2, 0^0\rangle$, and $|0, 2^{\pm 2}\rangle$. One can show that only the former two interactions contribute significantly to the A_1, A_2 splitting of the $kl = 1$ levels in the vibrational state $|1, 1^{\pm 1}\rangle$, yielding

$$\Delta_{\text{Cor}} = (2B\zeta_{3,6}^y \Omega_{3,6})^2 \{ [(\nu_3 + \nu_6) - 2\nu_6 + A - B - 2A\zeta_6^z]^{-1} + 2[(\nu_3 + \nu_6) - 2\nu_3 + A - B - 2A\zeta_6^z]^{-1} \} J(J+1). \quad (11)$$

The energies of the vibrational states ν_6 , $(\nu_3 + \nu_6)$, and $2\nu_3$ are known (Table III); we

TABLE V

Wavenumbers/cm⁻¹ of Lines in the Band ν_3 of H₃¹²CF Recommended as Secondary Standards for Calibration

ASSIGNMENT	EXP	CALC	(EXP-CALC)/10 ⁻⁶	I ^a
P(42, 4)	958.498494	958.498482	12	0.02
P(40, 9)	963.563624	963.563627	-3	0.01
P(40, 6)	963.593099	963.593089	10	0.04
P(39, 7)	966.113219	966.113254	-35	0.02
P(39, 6)	966.119802	966.119772	30	0.05
P(30, 5)	987.983764	987.983775	-11	0.33
F(28, 5)	992.622912	992.622931	-19	0.50
F(28, 6)	992.629508	992.629547	-39	0.79
P(27, 5)	994.912003	994.912022	-19	0.61
P(26, 6)	997.189175	997.189202	-27	1.14
F(25, 4)	999.421044	999.421084	-40	1.06
F(25, 5)	999.428624	999.428660	-36	0.87
F(25, 6)	999.430123	999.430163	-40	1.36
P(25, 7)	999.449715	999.449747	-32	0.51
P(24, 5)	1001.655982	1001.655984	-2	1.02
F(24, 6)	1001.666391	1001.666395	-4	1.59
P(24, 7)	1001.679110	1001.679105	5	0.59
P(23, 4)	1003.853513	1003.853517	-4	1.45
P(23, 5)	1003.862490	1003.862498	-8	1.19
P(23, 6)	1003.873773	1003.873787	-14	1.85
F(23, 7)	1003.887596	1003.887585	11	0.69
P(23, 9)	1003.923804	1003.923774	30	0.66
P(22, 3)	1006.031090	1006.031122	-32	3.94
P(22, 4)	1006.038462	1006.038451	11	1.68
P(22, 5)	1006.048072	1006.048095	-23	1.37
F(22, 6)	1006.060204	1006.060228	-24	2.12
F(22, 7)	1006.075085	1006.075076	9	0.98
P(22, 8)	1006.092957	1006.092917	40	0.56
P(22, 9)	1006.114130	1006.114099	31	0.75
P(21, 4)	1008.202379	1008.202390	-11	1.91
P(21, 5)	1008.212653	1008.212669	-16	1.55
F(21, 6)	1008.225604	1008.225612	-8	2.41
F(21, 7)	1008.241475	1008.241465	10	0.89
F(21, 8)	1008.260546	1008.260538	8	0.63
F(21, 9)	1008.283228	1008.283212	16	0.84
P(20, 3)	1010.336958	1010.336972	-14	5.08
F(20, 4)	1010.345212	1010.345234	-22	2.16
P(20, 5)	1010.356114	1010.356118	-4	1.75
P(20, 6)	1010.369841	1010.369832	9	2.70
F(20, 7)	1010.386656	1010.386646	10	1.00
P(20, 8)	1010.406911	1010.406894	17	0.70
F(20, 9)	1010.431019	1010.430996	23	0.93
F(19, 5)	1012.478313	1012.478339	-26	1.95
F(19, 7)	1012.510501	1012.510511	-10	1.10
F(19, 8)	1012.531877	1012.531877	0	0.77
F(19, 9)	1012.557339	1012.557337	2	1.02
F(18, 4)	1014.567205	1014.567235	-30	2.65
F(18, 5)	1014.579236	1014.579233	3	2.14
F(18, 6)	1014.594383	1014.594370	13	2.08
P(18, 7)	1014.612996	1014.612956	40	1.20
F(18, 8)	1014.635410	1014.635380	30	0.83
F(18, 9)	1014.662136	1014.662125	11	1.09
P(17, 4)	1016.646182	1016.646200	-18	2.89
F(17, 5)	1016.658591	1016.658703	-12	2.32
P(17, 6)	1016.674477	1016.674487	-10	3.54
F(17, 7)	1016.693874	1016.693880	-6	1.28
P(17, 8)	1016.717283	1016.717296	-13	0.88
P(17, 9)	1016.745248	1016.745251	-3	1.15
F(16, 4)	1018.703710	1018.703683	27	3.11
F(16, 5)	1018.718671	1018.718655	16	2.48
F(16, 6)	1018.733056	1018.733039	17	3.76
F(16, 7)	1018.753179	1018.753183	-4	1.35
F(16, 8)	1018.777532	1018.777525	8	0.92
F(16, 9)	1018.806605	1018.806609	-4	1.18
F(15, 4)	1020.739588	1020.739593	-5	0.30
F(15, 5)	1020.753008	1020.752995	13	2.62
F(15, 6)	1020.769917	1020.769932	-15	3.94
F(15, 7)	1020.790759	1020.790768	-9	1.40
F(15, 8)	1020.815959	1020.815965	-6	0.94
F(15, 9)	1020.846064	1020.846095	-31	1.28
F(14, 4)	1022.753841	1022.753840	1	3.44
P(14, 5)	1022.767632	1022.767633	-1	2.72
F(14, 6)	1022.785048	1022.785073	-25	4.05
F(14, 7)	1022.806537	1022.806542	-5	1.42
F(14, 8)	1022.832514	1022.832521	-7	0.93
F(14, 9)	1022.863589	1022.863610	-21	1.14
P(13, 4)	1024.746372	1024.746339	33	3.54
F(13, 5)	1024.760491	1024.760483	8	2.77
P(13, 6)	1024.778375	1024.778375	0	4.07
F(13, 7)	1024.800431	1024.800413	18	1.40
F(13, 8)	1024.827097	1024.827098	-1	0.90
F(13, 9)	1024.859036	1024.859056	-20	1.06
P(12, 2)	1026.698418	1026.698429	-11	5.02
P(12, 3)	1026.706108	1026.706075	33	8.72
F(12, 4)	1026.716575	1026.717007	-32	3.58
P(12, 5)	1026.731423	1026.731459	-36	2.76
P(12, 6)	1026.749729	1026.749750	-21	3.99
F(12, 7)	1026.772269	1026.772292	-23	1.34
F(12, 8)	1026.799572	1026.799605	-33	0.83
F(11, 4)	1028.665754	1028.665761	-7	3.54
F(11, 5)	1028.680452	1028.680478	-26	2.68
F(11, 6)	1028.699120	1028.699113	7	3.78
F(11, 7)	1028.722081	1028.722093	-12	1.22
F(11, 8)	1028.749925	1028.749954	-29	0.71
F(10, 4)	1030.592507	1030.592523	-16	3.41

^a Relative intensities appropriate for 300 K on a scale 0–10.

TABLE V—Continued

ASSIGNMENT	EXP	CALC	(EXP-CALC)/10 ⁻⁶	I ^a
P(10, 5)	1030.607438	1030.607461	-23	2.53
P(10, 6)	1030.626394	1030.626385	9	3.43
P(10, 7)	1030.649728	1030.649733	-5	1.04
P(10, 8)	1030.678054	1030.678060	-6	0.54
P(9, 4)	1032.497186	1032.497217	-31	3.19
P(9, 5)	1032.512398	1032.512350	-48	2.28
P(9, 6)	1032.531465	1032.531485	-20	2.92
P(9, 7)	1032.555137	1032.555133	4	0.79
F(8, 5)	1034.395004	1034.395012	-8	1.92
F(8, 6)	1034.414333	1034.414340	-7	2.20
F(7, 4)	1036.240086	1036.240111	-25	2.40
F(7, 5)	1036.255453	1036.255435	18	1.45
F(7, 6)	1036.274874	1036.274876	-2	1.25
F(6, 3)	1038.066563	1038.066585	-22	5.62
F(6, 4)	1038.078163	1038.078173	-10	1.80
F(6, 5)	1038.093547	1038.093530	17	0.82
F(5, 3)	1039.882307	1039.882318	-11	4.20
F(5, 4)	1039.893861	1039.893889	-28	1.02
F(4, 3)	1041.675603	1041.675600	3	2.40
Q(20, 6)	1043.904486	1043.904478	8	0.54
Q(19, 6)	1044.356278	1044.356290	-12	0.67
Q(19, 9)	1044.391329	1044.391297	32	0.59
Q(17, 6)	1045.193195	1045.193168	27	1.01
Q(17, 7)	1045.204958	1045.204937	21	0.52
Q(17, 9)	1045.237405	1045.237367	38	0.89
Q(16, 3)	1045.553766	1045.553768	-2	0.54
Q(16, 5)	1045.567816	1045.567801	15	0.54
Q(16, 6)	1045.581337	1045.578129	8	1.23
Q(16, 7)	1045.591099	1045.591082	17	0.64
Q(16, 8)	1045.607076	1045.607079	-3	0.61
Q(16, 9)	1045.626643	1045.626639	4	1.09
Q(15, 3)	1045.914455	1045.914441	4	0.65
Q(15, 4)	1045.929715	1045.920693	22	0.73
Q(15, 5)	1045.929472	1045.929458	14	0.65
Q(15, 7)	1045.954788	1045.954787	1	0.77
Q(15, 8)	1045.972178	1045.972144	34	0.74
Q(15, 9)	1045.993345	1045.993324	21	1.32
Q(15, 10)	1046.018980	1046.019004	-24	0.55
Q(14, 3)	1046.252232	1046.252197	35	0.79
Q(14, 4)	1046.259298	1046.259275	23	0.61
Q(14, 5)	1046.268768	1046.268733	35	0.79
Q(14, 6)	1046.280876	1046.280853	23	1.80
Q(14, 8)	1046.314675	1046.314651	24	0.90
Q(14, 9)	1046.337388	1046.337369	19	1.59
Q(14, 10)	1046.364853	1046.364868	-15	0.66
Q(14, 11)	1046.397982	1046.398015	-33	0.52
Q(14, 12)	1046.437822	1046.437861	-39	0.77
Q(13, 3)	1046.567933	1046.567898	35	0.95
Q(13, 4)	1046.575498	1046.575472	26	0.73
Q(13, 5)	1046.585607	1046.585583	24	0.95
Q(13, 6)	1046.598551	1046.598526	25	2.17
Q(13, 7)	1046.614723	1046.614687	36	1.13
Q(13, 8)	1046.634574	1046.634551	23	1.08
Q(13, 9)	1046.658725	1046.658720	5	1.92
Q(13, 10)	1046.687930	1046.687937	-7	0.80
Q(12, 3)	1046.861228	1046.861207	21	1.14
Q(12, 4)	1046.869247	1046.869246	1	0.88
Q(12, 5)	1046.879993	1046.879969	24	1.14
Q(12, 6)	1046.893586	1046.893685	1	2.61
Q(12, 7)	1046.910800	1046.910793	7	1.35
Q(12, 8)	1046.931823	1046.931798	25	1.30
Q(12, 9)	1046.957297	1046.957329	-32	2.31
Q(11, 3)	1047.132110	1047.132088	22	1.37
Q(11, 4)	1047.140564	1047.140561	3	1.05
Q(11, 5)	1047.151863	1047.151855	8	1.36
Q(11, 6)	1047.166283	1047.166290	-7	0.32
Q(11, 7)	1047.184283	1047.184281	2	1.62
Q(11, 8)	1047.206330	1047.206350	-20	1.55
Q(10, 3)	1047.380518	1047.380511	7	1.64
Q(10, 4)	1047.389376	1047.389385	-9	1.26
Q(10, 5)	1047.401206	1047.401206	0	1.63
Q(10, 6)	1047.416303	1047.416306	-3	3.75
Q(10, 7)	1047.435141	1047.435113	28	1.95
Q(10, 8)	1047.458160	1047.458166	-6	1.86
Q(9, 3)	1047.606478	1047.606446	32	1.97
Q(9, 4)	1047.615703	1047.615686	17	1.51
Q(9, 5)	1047.627997	1047.627991	6	1.96
Q(9, 6)	1047.643702	1047.643700	2	4.50
Q(9, 7)	1047.663247	1047.663254	-7	2.34
Q(9, 8)	1047.687201	1047.687209	-8	2.24
Q(9, 9)	1047.716230	1047.716256	-26	3.98
Q(8, 3)	1047.809888	1047.809865	23	2.37
Q(8, 4)	1047.819474	1047.819438	36	1.82
Q(8, 5)	1047.832207	1047.832181	26	2.36
Q(8, 6)	1047.848463	1047.848442	21	5.41
Q(8, 7)	1047.868662	1047.868674	-12	2.81
Q(8, 8)	1047.891453	1047.893446	7	2.69
Q(7, 3)	1047.990761	1047.990744	17	2.87
Q(7, 4)	1048.000628	1048.000614	14	2.21
Q(7, 5)	1048.013770	1048.013749	21	2.86
Q(7, 7)	1048.051347	1048.051342	5	3.41
Q(6, 2)	1048.142013	1048.142008	5	0.57
Q(6, 3)	1048.149042	1048.149061	-19	3.51
Q(6, 4)	1048.159216	1048.159193	23	2.70
Q(6, 5)	1048.172702	1048.172673	29	3.50
Q(5, 3)	1048.284773	1048.284798	-25	4.37
Q(5, 4)	1048.298163	1048.298155	8	3.16
Q(5, 5)	1048.308927	1048.308931	-4	4.35
Q(4, 3)	1048.397914	1048.397936	-22	5.59
Q(4, 4)	1048.408479	1048.408482	-3	4.29

TABLE V—Continued

ASSIGNMENT	EXP	CALC	(EXP-CALC) / 10 ⁻⁶	τ ^a
Q(3, 2)	1048.480998	1048.481015	-17	1.84
Q(3, 3)	1048.488433	1048.488464	-31	7.48
Q(1, 1)	1048.589600	1048.589589	11	1.32
R(3, 2)	1055.210740	1055.210721	19	2.51
R(4, 3)	1056.800399	1056.800416	-17	4.45
R(4, 4)	1056.809781	1056.809748	33	1.08
R(5, 4)	1058.376153	1058.376175	-22	1.93
R(5, 5)	1058.388092	1058.388074	18	0.88
R(6, 4)	1059.919669	1059.919696	-27	2.60
R(6, 5)	1059.930988	1059.930987	1	1.57
R(6, 6)	1059.945502	1059.945493	11	1.35
R(7, 4)	1061.440299	1061.440281	18	3.13
R(7, 5)	1061.450942	1061.450917	25	2.11
R(7, 6)	1061.464606	1061.464606	0	2.41
R(8, 4)	1062.937932	1062.937906	26	3.53
R(8, 5)	1062.947822	1062.947841	-19	2.52
R(8, 6)	1062.960668	1062.960657	11	3.28
R(8, 7)	1062.976812	1062.976795	17	0.88
R(9, 5)	1064.421743	1064.421736	7	2.83
R(9, 6)	1064.433624	1064.433622	2	3.85
R(9, 7)	1064.448648	1064.448634	14	1.17
R(9, 8)	1064.467295	1064.467315	-20	3.04
R(10, 5)	1065.872562	1065.872583	-21	3.04
R(10, 6)	1065.883491	1065.883483	8	4.29
R(10, 7)	1065.897216	1065.897200	16	1.39
R(10, 8)	1065.914571	1065.914562	9	0.80
R(10, 9)	1065.935887	1065.935920	-33	0.79
R(11, 4)	1067.292785	1067.292801	-16	4.10
R(11, 5)	1067.300367	1067.300366	1	3.16
R(11, 6)	1067.310209	1067.310225	-16	4.57
R(11, 7)	1067.322809	1067.322782	27	1.54
R(11, 8)	1067.338521	1067.338543	8	0.95
R(11, 9)	1067.358130	1067.358140	-10	1.05
R(12, 5)	1068.705066	1068.705069	-3	3.21
R(12, 6)	1068.713808	1068.713836	-28	4.72
R(12, 7)	1068.725094	1068.725067	27	1.63
R(12, 8)	1068.739258	1068.739251	7	1.04
R(12, 9)	1068.756989	1068.756993	-4	1.23
R(13, 5)	1070.086651	1070.086682	-31	1.18
R(13, 6)	1070.094317	1070.094306	11	4.74
R(13, 9)	1070.132499	1070.132479	20	1.34
R(14, 6)	1071.451606	1071.451627	-21	4.67
R(14, 7)	1071.460026	1071.460023	3	1.66
R(14, 9)	1071.484638	1071.484598	40	1.40
R(15, 6)	1072.785787	1072.785796	-9	4.52
R(17, 8)	1075.393633	1075.393610	23	1.02
R(18, 9)	1076.659560	1076.659526	34	1.26
R(23, 7)	1082.618960	1082.618950	10	0.78
R(23, 6)	1082.625886	1082.625875	11	2.09
R(24, 7)	1083.743024	1083.743012	12	0.67
R(24, 6)	1083.751850	1083.751845	5	1.80
R(24, 5)	1083.759616	1083.759593	23	1.15
R(24, 4)	1083.766124	1083.766116	8	1.41
R(25, 9)	1084.818769	1084.818732	37	0.56
R(25, 7)	1084.843950	1084.843968	-18	0.58
R(25, 6)	1084.854719	1084.854739	-20	1.54
R(25, 5)	1084.864076	1084.864081	-5	0.98
R(25, 4)	1084.871916	1084.871881	35	1.20
R(26, 6)	1085.945500	1085.945474	-24	1.30
R(26, 5)	1085.945538	1085.945535	3	0.83
R(26, 4)	1085.954647	1085.954630	17	1.01
R(27, 6)	1086.991345	1086.991371	-26	1.09
R(27, 5)	1087.003976	1087.003971	5	0.69
R(27, 4)	1087.014412	1087.014378	34	0.84
R(27, 3)	1087.022573	1087.022536	37	1.97
R(28, 6)	1088.025117	1088.025150	-33	0.90
R(28, 5)	1088.039393	1088.039407	-14	0.57
R(28, 4)	1088.051161	1088.051142	19	0.70
R(28, 3)	1088.060352	1088.060315	37	1.63
R(29, 4)	1089.064914	1089.064940	-6	0.57
R(29, 3)	1089.075171	1089.075140	31	1.33
R(30, 6)	1090.023723	1090.023745	-22	0.66
R(30, 5)	1090.041373	1090.041363	10	0.38
R(30, 4)	1090.055827	1090.055791	36	0.46
R(31, 5)	1091.007927	1091.007926	1	0.31
R(31, 4)	1091.021718	1091.020717	21	0.37
R(31, 3)	1091.036030	1091.035998	32	0.87
R(32, 5)	1091.951540	1091.951575	-35	0.24
R(32, 3)	1091.982099	1091.982072	27	0.69
R(33, 4)	1092.890891	1092.890881	10	0.23
R(34, 7)	1093.716660	1093.716661	-1	0.05
R(34, 6)	1093.745730	1093.745767	-37	0.24
R(34, 5)	1093.770208	1093.770235	-27	0.15
R(34, 4)	1093.790169	1093.790165	4	0.18
R(34, 3)	1093.805619	1093.805619	0	0.43
R(35, 6)	1094.639069	1094.639099	-30	0.19
R(35, 5)	1094.645304	1094.645296	8	0.32
R(35, 4)	1094.666584	1094.666616	-32	0.14
R(35, 3)	1094.694943	1094.694913	30	0.18
R(36, 5)	1095.497543	1095.497547	-4	0.09
R(37, 7)	1096.261944	1096.261975	-31	0.04
R(37, 4)	1096.351161	1096.351127	34	0.08
R(37, 3)	1096.369834	1096.369797	37	0.19
R(38, 5)	1097.133764	1097.133727	37	0.05
R(38, 4)	1097.159278	1097.159240	38	0.06

estimate $2\nu_6 = (2350 \pm 5) \text{ cm}^{-1}$. Thus

$$\Delta_{\text{Cor}} = 1.842 \times 10^{-3} J(J+1) \quad (12)$$

compared to the value derived from Table III,

$$\Delta_{\text{exp}} = -7.155 \times 10^{-5} J(J+1), \quad (13)$$

which gives for the state $|1, 1^{\pm 1}\rangle$

$$\Delta_{2,2} = -1.913 \times 10^{-3} J(J+1) \quad (14)$$

in good agreement with the value of $\Delta_{2,2}$ for the state $|0, 1^{\pm 1}\rangle$ in Eq. (10).

CONCLUSION

The weighted fit of almost 2300 lines in total within three vibration-rotational bands, together with 150 lines for pure rotational transitions, to only 42 parameters (total for the three bands) with a standard deviation either 5.6×10^{-5} or 7.6×10^{-5} cm^{-1} , or about 1/30 times the spectral resolution, clearly demonstrates satisfactory spectral measurements and analysis. Instead of presenting as part of this printed paper the extensive tables of the measured and calculated wavenumbers of the various bands, in Table V in order of increasing wavenumber in the range 958–1097 cm^{-1} we have listed 290 lines of the ν_3 band which we recommend as secondary standards for wavenumber calibration with accuracy exceeding 10^{-4} cm^{-1} . We selected these lines on the basis of their quality (isolated lines with good ratio of signal to noise), using the criterion $|\nu_{\text{exp}} - \nu_{\text{calc}}| \leq 4 \times 10^{-5}$ cm^{-1} . The relative intensities of the lines indicated in the last column of Table V were calculated by means of a standard formula for the intensities of unperturbed lines (13); except at the extremities of the band, an additional criterion to include lines in Table V was that their relative intensities exceed 5% of the most intense line. A complete list of the wavenumbers of the lines of the three bands ν_3 , $2\nu_3 - \nu_3$, and $\nu_3 + \nu_6 - \nu_6$ has been deposited in the editorial office of this journal and is available from the authors.

ACKNOWLEDGMENTS

We are indebted to Dr. J. Pola (Prague) and Dr. R. Fajgar (Prague) for help in preparing the sample of H₃CF and to K. Lattner (Giessen) for his expert assistance in recording the infrared spectra. The laboratory work carried out in Giessen was supported in part by the Deutsche Forschungsgemeinschaft and the Fonds der Chemischen Industrie. The authors thank Dr. B. P. Winnewisser for critically reading the manuscript. D.P. thanks the National Science Council of the Republic of China for appointment as visiting research professor at the Academia Sinica Institute of Atomic and Molecular Sciences, and the research of J.F.O. is also supported by the National Science Council of the Republic of China.

RECEIVED: April 12, 1991

REFERENCES

1. S. K. LEE, R. H. SCHWENDEMAN, R. L. CROWNOVER, D. D. SKATRUD, AND F. C. DELUCIA, *J. Mol. Spectrosc.* **123**, 145–160 (1987).
2. H. G. CHO, Y. MATSUO, AND R. H. SCHWENDEMAN, *J. Mol. Spectrosc.* **137**, 215–229 (1989).
3. W. F. EDGELL AND L. PARTS, *J. Am. Chem. Soc.* **77**, 4899–4902 (1955).

4. D. PAPOUŠEK, R. TESAŘ, P. PRACNA, S. CIVIŠ, M. WINNEWISSER, S. P. BELOV, AND M. YU. TRETYAKOV, *J. Mol. Spectrosc.* **147**, 279–299 (1991).
5. F. X. BROWN, D. DANGOISSE, J. GADHI, G. WŁODARCZAK, AND J. DEMAISON, *J. Mol. Struct.* **190**, 401–407 (1988).
6. D. PAPOUŠEK, P. PRACNA, R. TESAŘ, S. P. BELOV, AND M. YU. TRETYAKOV, *Vib. Spectrosc.*, **1**, 167–171 (1990).
7. D. PAPOUŠEK AND M. R. ALIEV, “Molecular Vibration–Rotational Spectra,” Elsevier and Academia, Amsterdam and Prague, 1982.
8. G. DI LONARDO, L. FUSINA, AND J. W. C. JOHNS, *J. Mol. Spectrosc.* **104**, 282–301 (1984).
9. G. GRANER, *Mol. Phys.* **31**, 1833–1843 (1976).
10. K. M. T. YAMADA, *Z. Naturforsch. A* **38**, 821–834 (1983).
11. C. DILAURO, F. LATTANZI, AND G. GRANER, *J. Mol. Spectrosc.* **143**, 111–136 (1990).
12. E. ARIMONDO AND M. INGUSCIO, *J. Mol. Spectrosc.* **75**, 81–86 (1979).
13. G. HERZBERG, “Molecular Spectra and Molecular Structure. II. Infrared and Raman Spectra of Polyatomic Molecules,” Van Nostrand, New York, 1945.